

## Drifting solitary waves in a reaction-diffusion medium with differential advection

Arik Yochelis\* and Moshe Sheintuch

Department of Chemical Engineering, Technion-Israel Institute of Technology, Haifa 32000, Israel  
(Received 15 May 2009; revised manuscript received 21 September 2009; published 8 February 2010)

A distinct propagation of solitary waves in the presence of autocatalysis, diffusion, and symmetry-breaking (differential) advection, is being studied. These pulses emerge at lower reaction rates of the autocatalytic activator, i.e., when the advective flow overcomes the fast excitation and induces a fluid type “drifting” behavior, making the phenomenon unique to reaction-diffusion-advection class systems. Using the spatial dynamics analysis of a canonical model, we present the properties and the organization of such drifting pulses. The insights underly a general understanding of localized transport in simple reaction-diffusion-advection models and thus provide a background to potential chemical and biological applications.

DOI: 10.1103/PhysRevE.81.025203

PACS number(s): 82.40.Ck, 47.35.Fg, 47.20.Ky

Solitary waves are prominent generic solutions to reaction-diffusion (RD) systems and basic to many applied science disciplines [1]. In one physical space dimension, these spatially localized propagating pulses are qualitatively described by a fast excitation (leading front) from a rest state followed by a slow recovery (rear front) to the same uniform state [1]. Thus, in isotropic RD media a single symmetric suprathreshold localized perturbation results in simultaneously *counterpropagating* pulses or wave trains [2].

However, in chemical and biological media transport can be facilitated by both diffusion and advection, and thus excitation properties of solitary waves can be subjected to linear and nonlinear convective instabilities [3]. Several experiments in a spatially quasi-one-dimensional Belousov-Zhabotinsky chemical reaction have shown (along with numerical simulations) that excitable pulses propagate against the advective flow [4,5] and can propagate bidirectionally after splitting due to the “antirefractory” phenomenon, triggered by the imposed electrical field [4]. In the latter case, the up- and down-stream traveling pulses retain the standard RD property of propagation by a fast excitation in the leading front. Consequently, the theoretical foundations of traveling and/or propagation failure of solitary waves in differential reaction-diffusion-advection (RDA) media, inherited the intuition of RD systems [6].

In this Rapid Communication we analyze an RDA model and demonstrate a distinct solitary wave phenomenon that cannot emerge in RD systems: under certain conditions solitary waves may *drift*; i.e., *the slow recovery becomes a leading front* (see Fig. 1). We reveal the regions and the properties of such drifting pulses and show that the phenomenon underlies a competition between a local kinetics of the activator and a differential advection. Our methods include a bifurcation theory of coexisting spatial solutions (linear analysis and numerical continuations) coupled to temporal stability; all the results agree well with direct numerical integrations. Applicability to chemical and biological media is also discussed.

We start with a canonical RDA model that incorporates local kinetics of activator  $v(x,t)$  and inhibitor  $u(x,t)$  type,

$$u_t + u_x = Da f(u,v) - u,$$

$$Le v_t + v_x = B Da f(u,v) - \alpha v + Pe^{-1} v_{xx}. \quad (1)$$

This is a general RDA model of membrane (or cross flow) reactor [7] that describes two species reacting at a rate  $f(u,v)$  in which reactants are supplied and products are removed at a rate of  $u$  and  $\alpha v$  for the two species, respectively. In the present case we choose the simple exothermic reaction described by Arrhenius kinetics. The latter is used for many reactor design problems, for understanding instabilities, explosions and cool flames [8]. In that case  $v$  is dimensionless temperature and  $f(u,v) \equiv (1-u)\exp[\gamma v/(\gamma+v)]$  [9].

Equation (1) admits uniform rest states  $(u,v) = (u_0, v_0) \equiv (Bu_0/\alpha)$ , where  $u_0$  obtained via  $Da = u_0(1-u_0)^{-1} \exp[-\gamma u_0/(\gamma\alpha/B + u_0)]$ . In what follows, we set  $Pe = 15$ ,  $\alpha = 4$ ,  $\gamma = 10\,000$ , and use  $Le$ ,  $Da$ , and  $B$  as control parameters allowed to vary; details regarding the parameters are given in [10]. A standard linear stability analysis to spatially periodic perturbations [using Eq. (1)], shows that the uniform states may loose stability to two finite wavenumber Hopf instabilities,  $Da^\pm$ , that emerge from  $(B^W, Da^W)$ , as shown in Fig. 1; the instabilities are of an asymmetric drifting type, i.e., in direction of advection. While the region  $Da^- < Da < Da^+$  is linearly unstable, under certain conditions stationary periodic (SP) solutions may also develop (see dotted line in Fig. 1). For more details about these instabilities and the effect of boundary conditions we refer the reader to [10]. Here, our interest is in the effect of a differential advection ( $Le$ ) and the local kinetics ( $B, Da$ ) on the organization of solitary waves. We also consider large domains in which pulse properties is not determined by the type of boundary conditions (periodic, no flux, or Robin) nor we are interested in the regimes in which nonuniform steady-state patterns may form.

To reveal the propagation properties and the regimes of solitary waves (see Fig. 1), we look at the steady-state version of Eq. (1) in a traveling (comoving) coordinate,  $\xi = x - ct$ ,

$$u_\xi = [Da f(u,v) - u]/(1-c), \quad v_\xi = w,$$

$$w_\xi = Pe[(1-c)Le w - B Da f(u,v) + \alpha v]. \quad (2)$$

Using Eq. (2), the existence of nonuniform states can be analyzed via spatial dynamics methods, i.e., where space is

\*Present address: Landa Labs, P.O. Box 4060, Nes Ziona 74140, Israel. Email: arik.yochelis@landalabs.com

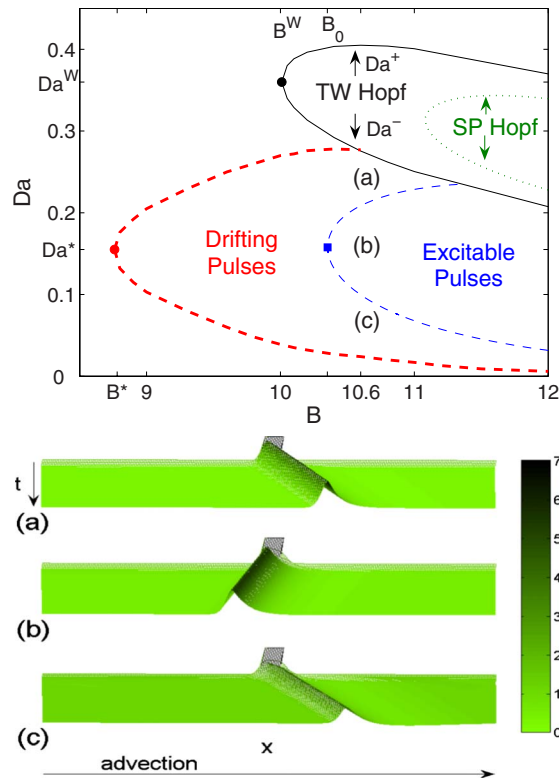


FIG. 1. (Color online) Top panel: regions of excitable (thick dashed line) and drifting (thin dashed line) solitary waves (pulses) in a parameter space  $(B, Da)$  at  $Le=100$ ; the thin dashed line implies zero velocity of a pulse. The solid line marks the onsets of finite wavenumber instabilities of traveling waves,  $TW^\pm$ . The dotted line marks the criterion for stationary patterns (SP) solutions (see text for details). The  $(\bullet)$ , marks the leftmost limits of homoclinic orbits  $(B^*, Da^*) \approx (8.76, 0.155)$  and asymmetric finite wavenumber Hopf bifurcation  $(B^W, Da^W) \approx (10, 0.36)$  while  $(\blacksquare)$  marks the leftmost limit of excitable pulses  $(B_0, Da^*) \approx (10.35, 0.155)$ . Bottom panel: space-time plots at  $B=10.6$  and (a)  $Da=0.24$ , (b)  $Da=0.15$ , and (c)  $Da=0.08$ . The plots show  $v(x, t)$  resulting from integration of Eq. (1) with no-flux boundary conditions, where  $x \in [0, 10]$  and  $t \in [0, 2265]$ ; we used a top-hat initial condition embedded in  $(u_0, v_0)$  at the respective  $Da$  values.

viewed as a timelike variable. Thus, solitary waves [in the context of Eq. (1)] become in Eq. (2) asymmetric homoclinic orbits (HOs) and  $TW^\pm$  (which will be also discussed) correspond to periodic orbits undergoing Hopf bifurcations at  $Da^\pm$  (with a proper  $c$ ) [10]. In the following all these solutions will be computed numerically using a continuation package AUTO [11], where the speed  $c$  is obtained as a nonlinear eigenvalue problem.

From physicochemical reasoning, the drifting pulses are expected at low reaction-rate regimes of the activator, represented in Eq. (1) by low dimensionless rate constant ( $Da$ ) and low exothermicity ( $B$ ). Under such conditions the excitation of nearest neighbors is suppressed due to the advective flow, hereafter, the drifting pulse is no longer excitable since the leading front now develops from the rest state as a *small* amplitude perturbation. These spatially slow deviations from the rest state are enhanced and propagate from  $x=0$  to  $x=L$ , due to the convective instability [3].

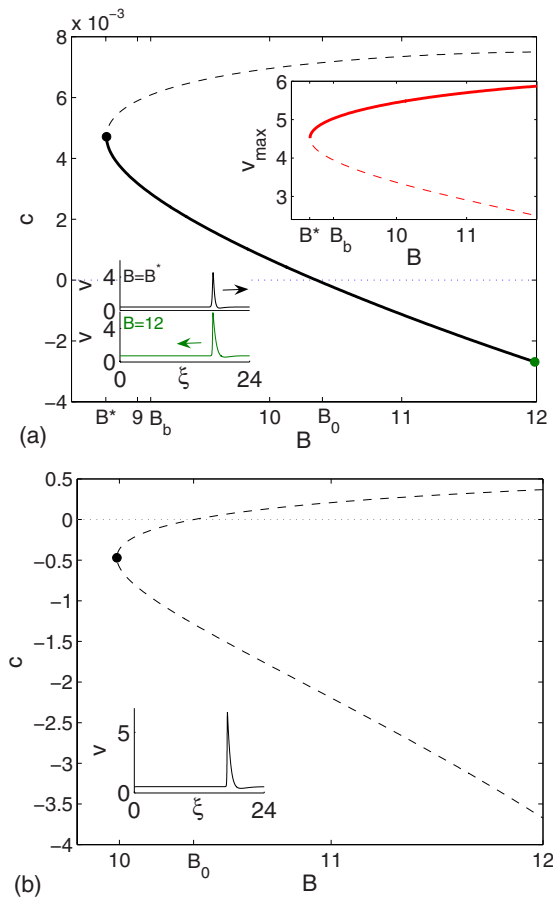


FIG. 2. (Color online) Bifurcation diagrams showing the branches of homoclinic solutions as a function of  $B$  at  $Da^* \approx 0.155$ ,  $Le=100$  (a), and  $Le=1$  (b). The branches are plotted in terms of the propagation speed and the maximal value of  $v(\xi)$  [top inset in (a)]; solid lines indicate linear stability. Bottom insets show profiles of  $v(\xi)$  at the locations marked by  $(\bullet)$ . The arrows in (a) indicate the propagation direction in the context of Eq. (1); in (b) the propagation is to the left. The branches were obtained via integration of Eq. (2) while the stable portions of each branch coincide with solutions obtained by integration of Eq. (1); the periodic domain is  $L=24$  (larger domains yield identical results).

In Fig. 2(a), we present the branches of HOs at  $Da=Da^* \approx 0.155$  (a horizontal cut in top panel in Fig. 1), resulting via a simultaneous variation of  $(B, c)$ .  $B=B^* \approx 8.76$  identifies a fold, where the stable branch corresponds to large amplitude HOs (see top inset). Indeed the drifting pulses exist for  $B^* < B < B_0 \approx 10.35$ , and have similar profiles along the stable branch as the standard excitable pulses (see bottom inset). Namely, drifting pulses propagate in the direction of the advection (downstream,  $c > 0$ ) where the leading region is now the slow recovery that was the trailing tail above  $B=B_0$  for excitable (upstream,  $c < 0$ ) pulses, as shown in the bottom inset in Fig. 2(a). This is qualitatively different from a typical RD behavior where the pulses always propagate with a fast excitation at the leading front [1,6].

The above scenario changes once the differential advection is eliminated ( $Le=1$ ) so that the typical RD behavior is restored. While the  $c=0$  line for  $Le=1$ , in the  $(B, Da)$  plane does not change, we show in Fig. 2(b) that near the fold only

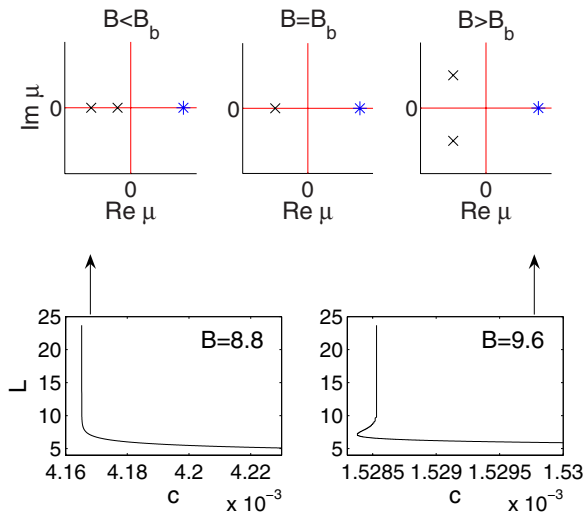


FIG. 3. (Color online) Top panel: schematic representation of typical eigenvalue configurations about the uniform state  $(u_0, v_0, 0)$  corresponding to a saddle if  $B < B_b$  and a saddle focus if  $B > B_b$ , where  $B_b \approx 9.1$  is the Belyakov point. Bottom panel: Typical dispersion relations that are associated with the respective eigenvalues, computed from the stable (drifting type) homoclinic orbits as a starting point. Parameters as in Fig. 2(a).

a negative velocity region forms, i.e., standard excitable pulses are being restored. Importantly, since solitary waves are “large” amplitude solutions (corresponding to the bottom branch), stability of the pulses does not play a qualitative role, i.e., due to the negative speed at the fold drifting pulses cannot emerge even when stabilized.

Since HOs arise in global bifurcations [15], we wish to uncover other type of stable coexisting solutions that may emerge in their vicinity.

As demonstrated by the monotonic and nonmonotonic dispersion relations in Fig. 3, drifting pulses appear to inherit

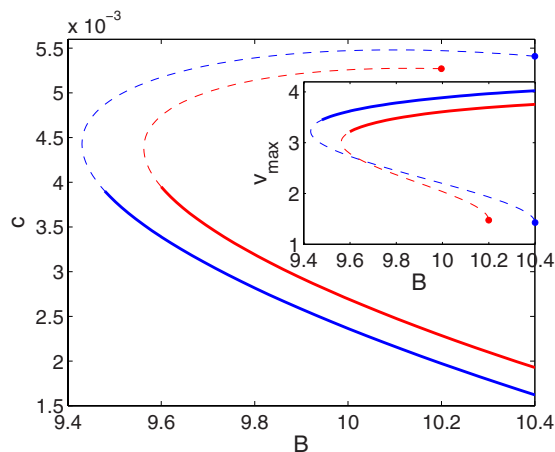


FIG. 4. (Color online) Bifurcation diagram showing the branches of traveling waves ( $TW^-$ ) as a function of  $B$  in terms of speed and the maximal value of  $v(\xi)$  (in the inset). The branches are continued from Hopf instabilities:  $(B, Da^-) \approx (10.4, 0.29)$  (left line) and  $(10.2, 0.29)$ , where  $(k_c, c) = (3.2, 0.0054)$  and  $(3.355, 0.0053)$ , respectively. Solid lines imply linear stability [12], while (●) marks the respective onsets of the Hopf bifurcation to  $TW^-$ . Integration details as in Fig. 2(a) but on  $L = 2\pi/k_c$ .

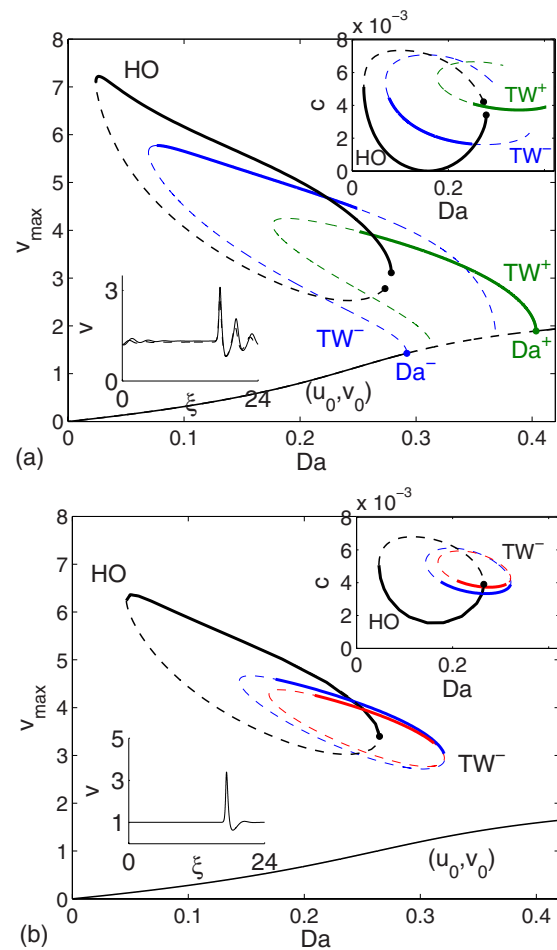


FIG. 5. (Color online) Bifurcation diagram showing the branches of uniform states  $(u_0, v_0)$ , homoclinic orbits (HOs), and traveling waves ( $TW^\pm$ ) as a function of  $Da$  in terms of the maximal value of  $v(\xi)$  at (a)  $B = 10.4$  and (b)  $B = 9.6$ . Solid lines imply linear stability, including stability of  $TW^\pm$  [12], while  $Da^\pm$  mark the onset Hopf bifurcations to  $TW^\pm$ , respectively. The top inset represents the nonuniform states in terms of speed where the large (small) isola in (b) corresponds to the  $TW^-$  family emerging from  $Da^-$  at  $B = 10.4$  ( $B = 10.2$ ). The bottom insets show HO profiles at locations marked by (●); in (a) the two dots mark also the two ends of the single pulse solitary wave branch. Integration details as in Fig. 2(a) but on distinct periodic domains.

the properties of excitable pulses. The latter are important characteristics of organization and interaction of solitary waves [13], and are distinguished here around  $B = B_b \approx 9.1$ , a so-called Belyakov point [14]. At this point and with an appropriate speed, the spatial eigenvalues [of Eq. (2)] correspond to one positive real (associated with  $\xi \rightarrow -\infty$ ) and a degenerate pair of negative reals (associated with  $\xi \rightarrow \infty$ ). Below  $B_b$ , the degeneracy is removed but the eigenvalues remain negative reals (a saddle) while above  $B_b$  they become complex conjugated corresponding to a saddle focus (a Shil'nikov-type HOs [2,15,16]), marked by (×) in top panel in Fig. 3. Importantly, such an interchange of eigenvalues implies a transition from monotonic to oscillatory dispersion relation (Fig. 3) and a monotonic (in space) approach of the HOs to the fixed point as  $\xi \rightarrow \pm \infty$ , which implies coexistence of bounded-pulse states for  $B > B_b$  [13].

It is known that organization of HO can be accompanied by periodic solutions [2,16]. Here the dispersion relations obtained at  $B < B^W$  (Fig. 3), indeed imply existence of periodic orbits although the uniform state is linearly stable. These periodic solutions are in fact  $TW^-$  that bifurcate subcritically from the locus of points  $Da = Da^-$  for  $B > B^W$  [with distinct critical wavenumbers and speeds obtained from the linear analysis of Eq. (1)], as shown by two sample curves in Fig. 4. Notably, there are an infinite number of such  $TW^-$  families. Unlike the HO, on large domains stability of  $TW^-$  solutions does depend on domain size [12].

The organization of all drifting nonuniform solutions can be understood by varying  $Da$  at two representative  $B$  values. Figure 5(a), shows the bifurcation diagram of nonuniform solutions and their propagation speed at  $B = 10.4$ . The single pulse HO branch ends at the two rightmost ends (marked by dots), at which the profiles take the form of homoclinic tails (see bottom inset) [16]. Due to the proximity to the subcritical Hopf onset at  $Da^-$ , the two rightmost ends ever approach each other as domain ( $L$ ) is increased, and consequently, they inherit the propagation direction of the top and the bottom branches of  $TW^-$  as discussed in [10]. As  $B$  is decreased below  $B^W$  the HOs and the  $TW^-$  solutions organize in isolas and parts of their stability regions overlap [Fig. 5(b)], implying sensitivity to initial perturbations. Note that the oscillations of the right tail in the profile had decreased (see bottom inset), which is consistent with the approach toward the Belyakov point ( $B = B_b$ ).

We have showed that solitary waves can propagate bidirectionally *without changing their profile*, due to the competition between activator autocatalysis and the symmetry-breaking advection. Thus, we distinguish between excitable

(upstream) and drifting (downstream) propagations. The drifting pulses are triggered by a convective instability [3], in two ways: (i) suppression of the excitation at the fast ( $\xi \rightarrow -\infty$ ) front and (ii) enhancement of weak deviations at the slow ( $\xi \rightarrow \infty$ ) front. As such, this is a distinct fluid type behavior that results in systems of an RDA class and cannot emerge in RD systems. Throughout a bifurcation analysis of spatially extended steady states arising in a canonical RDA model, we revealed the properties and the organization of such drifting pulses. Since the results center on homoclinic orbits which are known to act as organizing centers of spatial solutions, qualitative applicability to systems with other properties is naturally anticipated.

Although only excitable type solitary waves have been observed experimentally in an autocatalytic RDA system [4,5], chemical media are the most natural setups to confirm our predictions and to explore technological directions. Moreover, theoretical insights explored here can be exploited to spatiotemporal study of biological systems that constitute diffusive and advective transports, examples include self-organized mobility of intracellular molecular aggregates (organelles) in eucaryotic cells [17] and vegetation patterns [18].

#### ACKNOWLEDGMENTS

This work was supported by the U.S.-Israel Binational Science Foundation (BSF). A.Y. was partially supported by the Center for Absorption in Science, Ministry of Immigrant Absorption, State of Israel and M.S. is a member of the Minerva Center of Nonlinear Dynamics and Complex Systems.

- 
- [1] E. Meron, Phys. Rep. **218**, 1 (1992); M. C. Cross and P. C. Hohenberg, Rev. Mod. Phys. **65**, 851 (1993).
- [2] A. Yochelis *et al.*, EPL **83**, 64005 (2008).
- [3] J. M. Chomaz, Phys. Rev. Lett. **69**, 1931 (1992).
- [4] H. Sevcíková, M. Marek, and S. C. Müller, Science **257**, 951 (1992).
- [5] M. Kærn and M. Menzinger, Phys. Rev. E **65**, 046202 (2002).
- [6] J. Kosek, H. Sevcíková, and M. Marek, J. Phys. Chem. **99**, 6889 (1995); A. Hagberg and E. Meron, Phys. Rev. E **57**, 299 (1998); I. Kiss *et al.*, Q. J. Mech. Appl. Math. **57**, 467 (2004).
- [7] Le (Lewis number) is the ratio of solid-to-fluid-phase heat capacities,  $Pe$  (Péclet number) is the ratio of convective to conductive enthalpy fluxes,  $Da$  (Damköhler number) is the low dimensionless rate constant, and  $B$  is a stoichiometric constant.
- [8] L. M. Pismen, *Patterns and Interfaces in Dissipative Dynamics* (Springer-Verlag, Berlin, Heidelberg, 2006).
- [9] O. Nekhamkina, B. Y. Rubinstein, and M. Sheintuch, AIChE J. **46**, 1632 (2000).
- [10] A. Yochelis and M. Sheintuch, Phys. Rev. E **80**, 056201 (2009); Phys. Chem. Chem. Phys. **11**, 9210 (2009).
- [11] E. Doedel *et al.*, AUTO2000: *Continuation and bifurcation software for ordinary differential equations (with HOMCONT)*, <http://indy.cs.concordia.ca/auto/>
- [12] Temporal stability of  $TW^\pm$  was computed for large periodic domains,  $L = n\lambda_c$ ,  $n > 1$ ,  $\lambda_c \equiv 2\pi/k_c$  (until the onset did not change with the integer  $n$ ), via a standard numerical eigenvalue method using Eq. (1) in a comoving frame.  $k_c$  is the critical wave number at the Hopf onset.
- [13] C. Elphick *et al.*, J. Theor. Biol. **146**, 249 (1990); M. Or-Guil, I. G. Kevrekidis, and M. Bär, Physica D **135**, 154 (2000); G. Röder *et al.*, Phys. Rev. E **75**, 036202 (2007).
- [14] L. A. Belyakov, Mat. Zametki **28**, 911 (1980).
- [15] P. Glendinning and C. T. Sparrow, J. Stat. Phys. **35**, 645 (1984); N. J. Balmforth, Annu. Rev. Fluid Mech. **27**, 335 (1995); Yu. A. Kuznetsov, *Elements of Applied Bifurcation Theory* (Springer-Verlag, NY, 1995).
- [16] J. Sneyd, A. LeBeaub, and D. Yule, Physica D **145**, 158 (2000); A. R. Champneys *et al.*, SIAM J. Appl. Dyn. Syst. **6**, 663 (2007).
- [17] D. A. Smith and R. M. Simmons, Biophys. J. **80**, 45 (2001); J. S. Berg and R. E. Cheney, Nat. Cell Biol. **4**, 246 (2002); M. A. Welte, Curr. Biol. **14**, R525 (2004).
- [18] F. Borgogno *et al.*, Rev. Geophys. **47**, RG1005 (2009).